ACADEMIC PRESS

Available online at www.sciencedirect.com

SCIENCE DIRECT®

Journal of Computational Physics 184 (2003) 422–434

JOURNAL OF COMPUTATIONAL PHYSICS

www.elsevier.com/locate/jcp

Viscosity of finite difference lattice Boltzmann models

Victor Sofonea [a,b], Robert F. Sekerka [b,*]

[a] *Laboratory for Numerical Simulation and Parallel Computing in Fluid Mechanics, Center for Fundamental and Advanced Technical Research, Romanian Academy, Bd. Mihai Viteazul 24, R-1900 Timişoara, Romania*

[b] *Department of Physics, Carnegie Mellon University, 6416 Wean Hall, Pittsburgh, PA 15213, USA*

Received 2 January 2002; received in revised form 28 June 2002; accepted 9 October 2002

Abstract

Two-dimensional finite difference lattice Boltzmann models for single-component fluids are discussed and the corresponding macroscopic equations for mass and momentum conservation are derived by performing a Chapman–Enskog expansion. In order to recover the correct mass equation, characteristic-based finite difference schemes should be associated with the forward Euler scheme for the time derivative, while the space centered and second-order upwind schemes should be associated to second-order schemes for the time derivative. In the incompressible limit, the characteristic based schemes lead to spurious numerical contributions to the apparent value of the kinematic viscosity in addition to the physical value that enters the Navier–Stokes equation. Formulae for these spurious numerical viscosities are in agreement with results of simulations for the decay of shear waves.

Keywords: Lattice Boltzmann; Finite difference schemes; Kinematic viscosity

1. Introduction

Lattice Boltzmann (LB) models are derived from the continuous Boltzmann equation with the collision term in the Bhatnagar–Gross–Krook (BGK) approximation [1,2] after convenient discretization of the phase space [3,4]. Classical two-dimensional (2D) LB models (see [5–8] and references therein) for isothermal two-component fluid systems (e.g., the so-called D2Q9 model [9]) use a discrete lattice $\mathscr{L}$ where particle distribution functions $f_i^\sigma(\mathbf{x},t)$ defined at each lattice node $\mathbf{x}\in\mathscr{L}$ are updated after each time-step δt in accordance to the following evolution equations:

$$f_i^\sigma(\mathbf{x}+\mathbf{e}_i,t+\delta t)=f_i^\sigma(\mathbf{x},t)-\frac{1}{\tau^\sigma}[f_i^\sigma(\mathbf{x},t)-f_i^{\sigma,\mathrm{eq}}(\mathbf{x},t)]\quad(\sigma=0,1;\ i=0,1,\ldots,8). \tag{1}$$

* Corresponding author. Tel.: +1-412-268-2362; fax: +1-412-681-0648.
E-mail addresses: sofonea@acad-tim.utt.ro (V. Sofonea), rs07@andrew.cmu.edu (R.F. Sekerka).

0021-9991/03/$ - see front matter
doi:10.1016/S0021-9991(02)00026-8

Here the distribution function $f_i^\sigma(\mathbf{x},t),\ \sigma=0,1$, is the probability of finding at node $\mathbf{x}\in\mathscr{L}$ a particle belonging to component σ having the velocity $\mathbf{e}_i$, $f_i^{\sigma,\mathrm{eq}}$ are the corresponding equilibrium distribution functions and τ^σ are relaxation times. The nine velocities are given by

$$\mathbf{e}_i=\begin{cases}0 & (i=0),\\ \left[\cos\frac{\pi(i-1)}{2},\sin\frac{\pi(i-1)}{2}\right]c & (i=1,\ldots,4),\\ \left[\cos\left(\frac{\pi}{4}+\frac{\pi(i-5)}{2}\right),\sin\left(\frac{\pi}{4}+\frac{\pi(i-5)}{2}\right)\right]\sqrt{2}c & (i=5,\ldots,8),\end{cases}\tag{2}$$

where the propagation speed c of particles moving between a lattice node and its nearest neighbors has the same value for both fluid components. The value of c is related to the lattice spacing δs through

$$\delta s=c\delta t.\tag{3}$$

In most simulations, the value of c, as well as the value of the time-step δt are usually set to 1, which results in a lattice spacing δs of unit length.

Recent investigations [3,4,10] resulted in a general procedure to construct lattice Boltzmann models for single-component fluids. This procedure starts from the Boltzmann equation and employs a discretization of the phase space. The application of this procedure to an isothermal two-component fluid system whose particles have different masses $m^\sigma\neq m^{\bar\sigma}$ ($\bar\sigma=1-\sigma,\ \sigma=0,1$) is inappropriate because these lead to two different values

$$c^\sigma=\sqrt{\frac{k_\mathrm{B}T}{\chi m^\sigma}}\quad(\sigma=0,1)\tag{4}$$

for the propagation speed c in (2). Here k_B is Boltzmann's constant, T is the fluid temperature and $\chi=1/3$ for the D2Q9 model [10]. The constant χ has different values for other LB models (e.g., $\chi=1/4$ for the D2Q7 model introduced in [9]).

Since (4) is a very general result derived from the requirement that the phase space discretization has to be done in such a way that hydrodynamic moments up to third order of the Boltzmann equation are preserved exactly for isothermal LB models, the relation (3) should be rejected for multicomponent fluid systems (e.g., two-component systems) in order to allow for the general case when thermal speeds are different because the masses of the component particles are *not* identical. This means that the discretization of the velocity space should not be related to the discretization of the coordinate space in a simple way, as in classical LB models defined by (1) and (3).

To overcome this problem, finite difference lattice Boltzmann models (FDLB) may be used [11–15]. In these models, the set of the classical LB evolution equations for a two-component fluid (1) is replaced by the set of $\mathscr{N}+1$ discretized Boltzmann equations ($\partial_t:=\partial/\partial t$):

$$\partial_t f_i^\sigma(\mathbf{x},t)+\mathbf{e}_i^\sigma\cdot\nabla f_i^\sigma(\mathbf{x},t)=-\frac{1}{\tau^\sigma}\left[f_i^\sigma(\mathbf{x},t)-f_i^{\sigma,\mathrm{eq}}(\mathbf{x},t)\right]\quad(\sigma=0,1;\ i=0,1,\ldots,\mathscr{N})\tag{5}$$

for all nodes $\mathbf{x}\in\mathscr{L}$ (note that we do not sum over repeated i subscripts in the equations above). When using a square lattice, $\mathscr{N}=8$ and the velocities $\mathbf{e}_i^\sigma$ are similar to those in the D2Q9 model

$$\mathbf{e}_i^\sigma=\begin{cases}0 & (i=0),\\ \left[\cos\frac{\pi(i-1)}{2},\sin\frac{\pi(i-1)}{2}\right]c^\sigma & (i=1,\ldots,4),\\ \left[\cos\left(\frac{\pi}{4}+\frac{\pi(i-5)}{2}\right),\sin\left(\frac{\pi}{4}+\frac{\pi(i-5)}{2}\right)\right]\sqrt{2}c^\sigma & (i=5,\ldots,8),\end{cases}\tag{6}$$

except the speeds c^σ $(\sigma = 0, 1)$ are given by (4) and thus, $|\mathbf{e}_i^\sigma| \neq |\mathbf{e}_i^{\bar{\sigma}}|$ for $m^\sigma \neq m^{\bar{\sigma}}$. When using a hexagonal lattice (D2Q7 model), $\mathscr{N} = 6$ and the velocities $\mathbf{e}_i^\sigma$ are

$$\mathbf{e}_i^\sigma = \begin{cases} 0 & (i = 0), \\ \left[\cos\frac{\pi(i-1)}{3}, \sin\frac{\pi(i-1)}{3}\right] c^\sigma & (i = 1, \ldots, 6). \end{cases} \tag{7}$$

Although the viscosity of each fluid component is controlled by the corresponding relaxation time τ, finite difference schemes for the $\mathbf{e}_i^\sigma \cdot \nabla$ operator in (5) may introduce a spurious numerical viscosity in addition to the physical viscosity in the Navier–Stokes equation. To clarify this subject, we discuss some first- and second-order finite difference schemes for a single-component fluid and provide a derivation of the apparent value of the kinematic viscosity for each case.

2. Finite difference lattice Boltzmann models

For convenience, we consider a single-component fluid whose particles have the mass m. In this case, we do not need the superscript $\sigma = 0, 1$ used for the two-component system in (5) and the LB evolution equations are

$$\partial_t f_i(\mathbf{x}, t) + \mathbf{e}_i \cdot \nabla f_i(\mathbf{x}, t) = -\frac{1}{\tau}[f_i(\mathbf{x}, t) - f_i^{\mathrm{eq}}(\mathbf{x}, t)] \quad (i = 0, 1, \ldots, \mathscr{N}), \tag{8}$$

where $\mathscr{N} = 8$ or $\mathscr{N} = 6$. As in classical LB models, the equilibrium distribution functions in (8) are given as series expansions in the local velocity $\mathbf{u} \equiv \mathbf{u}(\mathbf{x}, t)$

$$f_i^{\mathrm{eq}}(\mathbf{x}, t) = w_i n \left[1 + \frac{\mathbf{e}_i \cdot \mathbf{u}}{\chi c^2} + \frac{(\mathbf{e}_i \cdot \mathbf{u})^2}{2\chi^2 c^4} - \frac{\mathbf{u} \cdot \mathbf{u}}{2\chi c^2}\right] \quad (i = 0, 1, \ldots, \mathscr{N}), \tag{9}$$

where $n \equiv n(\mathbf{x}, t)$ is the local particle number density and $c = \sqrt{k_B T/\chi m}$ is the thermal speed. For the D2Q9 model, the weight factors w_i are

$$w_i = \begin{cases} \frac{4}{9} & (i = 0), \\ \frac{1}{9} & (i = 1, \ldots, 4), \\ \frac{1}{36} & (i = 5, \ldots, 8), \end{cases} \tag{10}$$

while for the D2Q7 model these factors are

$$w_i = \begin{cases} \frac{1}{2} & (i = 0), \\ \frac{1}{12} & (i = 1, \ldots, 6). \end{cases} \tag{11}$$

For both models, the Cartesian projections $e_{i\alpha} \equiv (\mathbf{e}_i)_\alpha$ $(i = 0, 1, \ldots, \mathscr{N};\ \alpha = x, y)$ of the velocities $\mathbf{e}_i$ satisfy the relations

$$\begin{aligned} &\sum_i w_i e_{i\alpha} = 0, \\ &\sum_i w_i e_{i\alpha} e_{i\beta} = \chi c^2 \delta_{\alpha\beta}, \\ &\sum_i w_i e_{i\alpha} e_{i\beta} e_{i\gamma} = 0, \\ &\sum_i w_i e_{i\alpha} e_{i\beta} e_{i\gamma} e_{i\delta} = \chi^2 c^4 (\delta_{\alpha\beta}\delta_{\gamma\delta} + \delta_{\beta\gamma}\delta_{\delta\alpha} + \delta_{\alpha\gamma}\delta_{\beta\delta}). \end{aligned} \tag{12}$$

Using the expression (9) of the equilibrium distribution functions, the following sums are easily computed:

$$\begin{aligned}
&\sum_i f_i^{\mathrm{eq}} = n,\\
&\sum_i e_{i\alpha} f_i^{\mathrm{eq}} = n u_\alpha,\\
&\sum_i e_{i\alpha} e_{i\beta} f_i^{\mathrm{eq}} = n[\chi c^2 \delta_{\alpha\beta} + u_\alpha u_\beta],\\
&\sum_i e_{i\alpha} e_{i\beta} e_{i\gamma} f_i^{\mathrm{eq}} = n\chi c^2 [\delta_{\alpha\beta} u_\gamma + \delta_{\beta\gamma} u_\alpha + \delta_{\gamma\alpha} u_\beta].
\end{aligned} \tag{13}$$

Here u_α $(\alpha = x, y)$ are the Cartesian components of the local velocity $\mathbf{u}(\mathbf{x}, t)$.

The set of phase space discretized Boltzmann equations (8) for the distribution functions $f_i \equiv f_i(\mathbf{x}, t)$ may be solved numerically by using an appropriate finite difference scheme defined on the lattice $\mathscr{L}$. When using a scheme based on characteristics, the forward Euler difference is used to compute the time derivative and the distribution functions are updated at each lattice node in accordance with

$$f_i(\mathbf{x}, t + \delta t) = f_i(\mathbf{x}, t) - \delta t\, \mathbf{e}_i \cdot \nabla f_i(\mathbf{x}, t) - \frac{\delta t}{\tau}[f_i(\mathbf{x}, t) - f_i^{\mathrm{eq}}(\mathbf{x}, t)]. \tag{14}$$

Two second-order schemes may be used to compute the time derivative in (8): the midpoint scheme

$$f_i(\mathbf{x}, t + \delta t) = f_i(\mathbf{x}, t - \delta t) - 2\delta t\, \mathbf{e}_i \cdot \nabla f_i(\mathbf{x}, t) - \frac{2\delta t}{\tau}[f_i(\mathbf{x}, t) - f_i^{\mathrm{eq}}(\mathbf{x}, t)] \tag{15}$$

or the Runge–Kutta scheme [14,16]

$$f_i(\mathbf{x}, t + \delta t) = f_i(\mathbf{x}, t) - \delta t\, \mathbf{e}_i \cdot \nabla f_i(\mathbf{x}, t + \delta t/2) - \tfrac{\delta t}{\tau}[f_i(\mathbf{x}, t + \delta t/2) - f_i^{\mathrm{eq}}(\mathbf{x}, t + \delta t/2)]. \tag{16}$$

There are several possibilities [16–18] to compute the term $\mathbf{e}_i \cdot \nabla f_i(\mathbf{x}, t)$ in hyperbolic equations like (8). For this purpose, we use the Cartesian projections $e_{i\alpha} \equiv (\mathbf{e}_i)_\alpha$ $(i = 0, 1, \ldots, \mathscr{N}; \alpha = x, y)$ of the velocities $\mathbf{e}_i$:

(a) *First-order upwind scheme*

$$\mathbf{e}_i \cdot \nabla f_i(\mathbf{x}, t) = \frac{c}{\delta s}[f_i(x, y, t) - f_i(x - \delta s e_{ix}/c, y - \delta s e_{iy}/c, t)]. \tag{17}$$

(b) *Space centered scheme*

$$\mathbf{e}_i \cdot \nabla f_i(\mathbf{x}, t) = \frac{c}{2\delta s}[f_i(x + \delta s e_{ix}/c, y + \delta s e_{iy}/c, t) - f(x - \delta s e_{ix}/c, y - \delta s e_{iy}/c, t)]. \tag{18}$$

(c) *Second-order upwind scheme*

$$\mathbf{e}_i \cdot \nabla f_i(\mathbf{x}, t) = \frac{c}{2\delta s}[3 f_i(x, y, t) - 4 f_i(x - \delta s e_{ix}/c, y - \delta s e_{iy}/c, t) + f(x - 2\delta s e_{ix}/c, y - 2\delta s e_{iy}/c, t)]. \tag{19}$$

(d) *Lax scheme* (*also called Lax–Friedrichs scheme*)

$$\begin{aligned}
\mathbf{e}_i \cdot \nabla f_i(\mathbf{x}, t) = \frac{1}{\delta t}\Bigg[& f_i(x, y, t) - \frac{1}{2}\left(1 - \frac{c\delta t}{\delta s}\right) f_i(x + \delta s e_{ix}/c, y + \delta s e_{iy}/c, t)\\
& - \frac{1}{2}\left(1 + \frac{c\delta t}{\delta s}\right) f_i(x - \delta s e_{ix}/c, y - \delta s e_{iy}/c, t)\Bigg].
\end{aligned} \tag{20}$$

(e) *Lax–Wendroff scheme*

$$e_i \cdot \nabla f_i(\mathbf{x},t) = \frac{c}{2\delta s}[f_i(x+\delta s e_{ix}/c, y+\delta s e_{iy}/c, t) - f(x-\delta s e_{ix}/c, y-\delta s e_{iy}/c, t)] - \frac{1}{2}\frac{c^2\delta t}{(\delta s)^2}[f_i(x+\delta s e_{ix}/c, y+\delta s e_{iy}/c, t) - 2f(x,y,t) + f(x-\delta s e_{ix}/c, y-\delta s e_{iy}/c, t)]. \tag{21}$$

(f) *Beam–Warming scheme*

$$\mathbf{e}_i \cdot \nabla f_i(\mathbf{x},t) = \frac{c}{2\delta s}\left[\left(3-\frac{c\delta t}{\delta s}\right)f_i(x,y,t) + \left(\frac{2c\delta t}{\delta s}-4\right)f_i(x-\delta s e_{ix}/c, y-\delta s e_{iy}/c, t) + \left(1-\frac{c\delta t}{\delta s}\right)f_i(x-2\delta s e_{ix}/c, y-2\delta s e_{iy}/c, t)\right]. \tag{22}$$

3. Physical viscosity and fluid equations

Two techniques may be used to derive the fluid equations from the Boltzmann equation (8): the method of moments of Grad [19–21] or the Chapman–Enskog expansion [5–8]. We will use the last approach and formally expand the distribution functions using a small parameter $\varepsilon = c\tau/L$ (the Knudsen number), where L is the system size

$$f_i \simeq f_i^{(0)} + \varepsilon f_i^{(1)} + \varepsilon^2 f_i^{(2)} + \cdots \tag{23}$$

Two time scales and one length scale are also adopted

$$t_1 = t\varepsilon, \tag{24}$$

$$t_2 = t\varepsilon^2, \tag{25}$$

$$\mathbf{r}_1 = \mathbf{r}\varepsilon, \tag{26}$$

such that the time and space derivative are expressed as

$$\partial_t = \varepsilon\partial_{t_1} + \varepsilon^2\partial_{t_2}, \tag{27}$$

$$\nabla_{\mathbf{r}} = \varepsilon\nabla_{\mathbf{r}_1} \tag{28}$$

(for convenience, we will use the notation $\partial_{\beta_1} := \partial/\partial x_{1\beta}$). The above expressions of the derivatives are substituted into Eq. (8) and terms involving ε to zeroth-, first- and second-order are separated to yield

$$0 = -\frac{1}{\tau}\left[f_i^{(0)} - f_i^{\mathrm{eq}}\right], \tag{29}$$

$$\partial_{t_1} f_i^{(0)} + e_{i\beta}\partial_{\beta_1} f_i^{(0)} = -\frac{1}{\tau} f_i^{(1)}, \tag{30}$$

$$\partial_{t_2} f_i^{(0)} + \partial_{t_1} f_i^{(1)} + e_{i\beta}\partial_{\beta_1} f_i^{(1)} = -\frac{1}{\tau} f_i^{(2)}. \tag{31}$$

From (29), we get

$$f_i^{(0)} = f_i^{\mathrm{eq}} \quad (i = 0, 1, \ldots, \mathcal{N}). \tag{32}$$

The zeroth-, first- and second-order mass conservation equations are recovered from Eqs. (29)–(31) after summation with respect to i (for convenience, multiplication with m is omitted here):

$$-\frac{1}{\tau}\sum_i \left[f_i^{(0)} - f_i^{\mathrm{eq}}\right] = 0, \tag{33}$$

$$\partial_{t_1}\sum_i f_i^{(0)} + \partial_{\beta_1}\sum_i f_i^{(0)} e_{i\beta} = -\frac{1}{\tau}\sum_i f_i^{(1)}, \tag{34}$$

$$\partial_{t_2}\sum_i f_i^{(0)} + \partial_{t_1}\sum_i f_i^{(1)} + \partial_{\beta_1}\sum_i f_i^{(1)} e_{i\beta} = -\frac{1}{\tau}\sum_i f_i^{(2)}. \tag{35}$$

The zeroth-, first- and second-order momentum conservation equations are recovered from Eqs. (29)–(31) after multiplication with $m\, e_{i\alpha}$ and summation with respect to i:

$$-\frac{1}{\tau}\sum_i m\left[f_i^{(0)} - f_i^{\mathrm{eq}}\right] e_{i\alpha} = 0, \tag{36}$$

$$\partial_{t_1}\sum_i m f_i^{(0)} e_{i\alpha} + \partial_{\beta_1}\sum_i m f_i^{(0)} e_{i\alpha} e_{i\beta} = -\frac{1}{\tau}\sum_i m f_i^{(1)} e_{i\alpha}, \tag{37}$$

$$\partial_{t_2}\sum_i m f_i^{(0)} e_{i\alpha} + \partial_{t_1}\sum_i m f_i^{(1)} e_{i\alpha} + \partial_{\beta_1}\sum_i m f_i^{(1)} e_{i\alpha} e_{i\beta} = -\frac{1}{\tau}\sum_i m f_i^{(2)} e_{i\alpha}. \tag{38}$$

The local particle number density n and the local velocity $\mathbf{u}$ are given by

$$n = \sum_i f_i = \sum_i f_i^{\mathrm{eq}}, \quad \mathbf{u} = \frac{1}{n}\sum_i f_i \mathbf{e}_i = \frac{1}{n}\sum_i f_i^{\mathrm{eq}} \mathbf{e}_i. \tag{39}$$

Thus, from the zeroth-order mass and momentum equations (33) and (36), we get

$$\sum_i f_i^{(l)} = 0, \quad \sum_i f_i^{(l)} \mathbf{e}_i = 0 \qquad \forall l \geqslant 1. \tag{40}$$

To recover the mass conservation equation up to second order with respect to the Knudsen number, we sum Eqs. (33)–(35) together after multiplication with ε^0, ε^1 and ε^2, respectively ($\rho = mn$):

$$\partial_t \rho + \partial_\beta(\rho u_\beta) = 0. \tag{41}$$

The Euler equation

$$\partial_{t_1}(\rho u_\alpha) + \partial_{\beta_1}(\rho u_\alpha u_\beta) = -\partial_{\alpha_1} p \tag{42}$$

is recovered from the first-order momentum equation (37) using Eqs. (13), (40), as well as the definition of the ideal gas pressure

$$p := n k_{\mathrm{B}} T = \chi c^2 \rho. \tag{43}$$

If we add the first- and second-order momentum equations (37) and (38), we get

$$\partial_t(\rho u_\alpha) + \partial_\beta \Pi_{\alpha\beta} = 0, \tag{44}$$

where the momentum flux density tensor $\Pi_{\alpha\beta}$ is given by

$$\Pi_{\alpha\beta} = \Pi^{(0)}_{\alpha\beta} + \varepsilon \Pi^{(1)}_{\alpha\beta}, \tag{45}$$

$$\Pi^{(0)}_{\alpha\beta} = m \sum_i e_{i\alpha} e_{i\beta} f_i^{(0)} = p\delta_{\alpha\beta} + \rho u_\alpha u_\beta, \tag{46}$$

$$\Pi^{(1)}_{\alpha\beta} = m \sum_i e_{i\alpha} e_{i\beta} f_i^{(1)} = -\tau n k_B T[\partial_{\alpha_1} u_\beta + \partial_{\beta_1} u_\alpha]. \tag{47}$$

To get the above expression of $\Pi^{(1)}_{\alpha\beta}$, we first express $f_i^{(1)}$ from (30) and use (13):

$$\Pi^{(1)}_{\alpha\beta} = -\tau \partial_{t_1}[\delta_{\alpha\beta} n k_B T + \rho u_\alpha u_\beta] - \tau k_B T[\delta_{\alpha\beta}\partial_{\gamma_1}(n u_\gamma) + \partial_{\alpha_1}(n u_\beta) + \partial_{\beta_1}(n u_\alpha)]. \tag{48}$$

Then we use the first-order mass and momentum equations (34) and (37) to get

$$\partial_{t_1}(n k_B T) = -k_B T \partial_{\gamma_1}(n u_\gamma), \tag{49}$$

$$\partial_{t_1}(\rho u_\alpha u_\beta) = -k_B T[u_\alpha \partial_{\beta_1} n + u_\beta \partial_{\alpha_1} n] - \partial_{\gamma_1}(\rho u_\alpha u_\beta u_\gamma), \tag{50}$$

$$\simeq -k_B T[u_\alpha \partial_{\beta_1} n + u_\beta \partial_{\alpha_1} n]. \tag{51}$$

The product $u_\alpha u_\beta u_\gamma$ is neglected since the LB model and the series expansion (9) are valid only for small Mach number ($u/c \ll 1$).

The final form of the momentum equation (44) is

$$\partial_t(\rho u_\alpha) + \partial_\beta(\rho u_\alpha u_\beta) = -\partial_\alpha p + \nu \partial_\beta[\rho \partial_\alpha u_\beta + \rho \partial_\beta u_\alpha]. \tag{52}$$

The Navier–Stokes equation is recovered from this equation in the incompressible limit ($\partial_\beta u_\beta = 0$)

$$\partial_t u_\alpha + u_\beta \partial_\beta u_\alpha = -\frac{1}{\rho}\partial_\alpha p + \nu \nabla^2 u_\alpha. \tag{53}$$

Here ν is the *physical value* of the kinematic viscosity of the single-component fluid

$$\nu = \tau \chi c^2 = \tau k_B T/m. \tag{54}$$

The above expression of the kinematic viscosity, which can be derived also using the method of moments [20,21], is of principal importance since it expresses the fact that the behavior of the fluid we simulate with the LB model is independent of the discretization of the velocity space (i.e., independent of $\mathcal{N}$ or χ). However, the numerical scheme used in the LB model may introduce a spurious viscosity term that adds to the *physical value* (54), as seen in the following section.

4. Numerical viscosity and apparent viscosity of finite difference lattice Boltzmann models

After performing a series expansion up to second order in Eqs. (17)–(22), we get (for convenience, simply write f_i instead of $f_i(\mathbf{x}, t)$ and $\partial_\alpha := \partial/\partial x_\alpha$; summation over repeated Greek indices is understood):

$$\mathbf{e}_i \cdot \nabla f_i = e_{i\beta}\partial_\beta f_i - \psi e_{i\beta}e_{i\gamma}\partial_\beta\partial_\gamma f_i, \tag{55}$$

where the expression of the factor ψ is given in Table 1 for all schemes introduced in Section 2. A similar procedure may be considered for the finite difference schemes used to compute the time derivatives. This means that the *real* LB equations solved using the updating schemes (14) or (15) are, up to second order in the lattice spacing δs $(i = 0, 1, \ldots, \mathcal{N})$

$$\partial_t f_i + \theta\partial_t^2 f_i + \mathbf{e}_i \cdot \nabla f_i - \psi e_{i\beta}e_{i\gamma}\partial_\beta\partial_\gamma f_i = -\frac{1}{\tau}[f_i - f_i^{\mathrm{eq}}] \tag{56}$$

instead of Eqs. (8). The factor θ introduced in the equation above has the value $\theta = \delta t/2$ when the forward Euler scheme (14) is considered. This factor vanishes when the second-order scheme (15) is considered to compute the time evolution of the distribution functions.

To investigate the effect of the supplementary terms in (56), we refer to the previously discussed derivation of the mass and momentum equations from the Boltzmann equation. The zeroth and first-order LB equations (29), (30) remain unchanged when performing the Chapman–Enskog expansion, while the second-order equation (31) becomes, after using (30) to express the second-order time derivative,

$$\partial_{t_2} f_i^{(0)} + \left[1 - \frac{\theta}{\tau}\right]\partial_{t_1} f_i^{(1)} + \left[1 + \frac{\theta}{\tau}\right] e_{i\beta}\partial_{\beta_1} f_i^{(1)} - [\psi - \theta]e_{i\beta}e_{i\gamma_1}\partial_{\beta_1}\partial_{\gamma_1} f_i^{(0)} = -\frac{1}{\tau} f_i^{(2)}. \tag{57}$$

The same second-order LB equation as above (with $\theta = 0$) is recovered when using the Runge–Kutta updating scheme (16). This may be easily checked from the real LB equations solved using this scheme:

$$\begin{aligned}\partial_t f_i + \mathbf{e}_i \cdot \nabla f_i - \psi e_{i\beta}e_{i\gamma}\partial_\beta\partial_\gamma f_i = {} & \frac{\delta t}{2}\left[- \partial_t^2 f_i + e_{i\beta}e_{i\gamma}\partial_\beta\partial_\gamma f_i + \frac{1}{\tau}(e_{i\beta}\partial_\beta - \partial_t)(f_i - f_i^{\mathrm{eq}})\right] \\ & - \frac{\delta t}{8\tau}\partial_t^2[f_i - f_i^{\mathrm{eq}}] - \frac{1}{\tau}[f_i - f_i^{\mathrm{eq}}].\end{aligned} \tag{58}$$

Consequently, the general mass and momentum equations recovered using the finite difference schemes introduced in Section 2, are (up to second order in the Knudsen number ε):

$$\partial_t \rho + \partial_\beta(\rho u_\beta) - [\psi - \theta]\partial_\beta\partial_\gamma[\chi c^2\rho\delta_{\beta\gamma} + \rho u_\beta u_\gamma] = 0, \tag{59}$$

$$\partial_t(\rho u_\alpha) + \partial_\beta(\rho u_\alpha u_\beta) = -\partial_\alpha p + \chi c^2[\tau + \theta]\partial_\beta[\rho\partial_\alpha u_\beta + \rho\partial_\beta u_\alpha] + \chi c^2[\psi - \theta][2\partial_\alpha\partial_\beta(\rho u_\beta) + \nabla^2(\rho u_\alpha)]. \tag{60}$$

Table 1
Expressions of the factors ψ and $\psi - \theta$ which appear in Eqs. (56), (59) and (60), for all finite difference schemes introduced in Section 2

$\mathbf{e}_i \cdot \nabla$	ψ	$\psi - \theta$	
		Forward Euler (14) $\theta = \delta t/2$	Second-order schemes (15) and (16) $\theta = 0$
First-order upwind (17)	$\frac{\delta s}{2c}$	$\frac{1}{2}\left[\frac{\delta s}{c} - \delta t\right]^*$	$\frac{\delta s}{2c}$
Space centered (18)	0	$-\frac{\delta t}{2}$	0
Second-order upwind (19)	0	$-\frac{\delta t}{2}$	0
Lax (20)	$\frac{(\delta s)^2}{2c^2\delta t}$	$\frac{1}{2}\left[\frac{(\delta s)^2}{c^2\delta t} - \delta t\right]^*$	$\frac{(\delta s)^2}{2c^2\delta t}$
Lax–Wendroff (21)	$\frac{\delta t}{2}$	0	$\frac{\delta t}{2}$
Beam–Warming (22)	$\frac{\delta t}{2}$	0	$\frac{\delta t}{2}$

Expressions marked * vanish for CFL = 1. In the incompressible limit, the apparent viscosity is given by Eq. (62) in all cases.

For all finite difference schemes considered in Section 2, the correct mass equation is apparently recovered when

$$\psi = \theta. \tag{61}$$

However, in the incompressible limit ($\rho = constant$ and small Mach number, which means $u_\beta u_\gamma \simeq 0$), the correct mass equation is still recovered for $\psi \neq \theta$.

When the forward Euler scheme (14) is associated to the first-order upwind scheme (17) or the Lax scheme (20), condition (61) means that the Courant–Friedrichs–Levy number CFL $:= c\delta t/\delta s$ equals 1. As mentioned previously, this condition is always satisfied in the classical LB models. From Table 1 we see that Eq. (61) is automatically satisfied by the Lax–Wendroff (21) and Beam–Warming (22) schemes if associated to the Euler scheme (14), but cannot be satisfied by these two schemes (as well as by the first-order upwind and the Lax scheme) when associated to the second-order updating schemes (15) and (16). Alternatively, Eq. (61) is automatically satisfied when the space centered scheme (18) or the second-order upwind scheme (19) are associated only to the second-order time updating schemes (15) or (16).

If we consider the momentum equation in the incompressible limit, the Navier–Stokes equation (53) is recovered with the *apparent value* of the kinematic viscosity:

$$v = \chi c^2[\tau + \psi] = \frac{\tau k_B T}{m}[1 + \psi/\tau] \tag{62}$$

regardless of the updating procedure, Eq. (14), (15) or (16). Thus, the finite difference scheme used for the calculation of the space derivative in the LB evolution equations may generate a spurious *numerical viscosity* term $\chi c^2\psi$ which adds to the *physical value* (54) of the kinematic viscosity in the Navier–Stokes equation (53).

For the *first-order upwind scheme*, the apparent value of the viscosity

$$v = \chi c^2\left[\tau + \frac{\delta s}{2c}\right] \tag{63}$$

is linearly dependent on the lattice spacing and is always larger than the physical value (54). In particular, when CFL = 1 and (3) is satisfied, the apparent value of the kinematic viscosity becomes

$$v = \frac{1}{2}\chi c^2[2\tau + \delta t]. \tag{64}$$

If we rewrite (63) using the definition of the Knudsen number, we get

$$v = \tau\chi c^2\left[1 + \frac{\delta s}{2\varepsilon L}\right] = \tau\chi c^2\left[1 + \frac{1}{2\varepsilon N}\right] = \chi cL\left[\varepsilon + \frac{1}{2N}\right], \tag{65}$$

where $N = L/\delta s$ is the number of lattice nodes. Consequently, a large number of lattice nodes N (i.e., a huge computing effort, especially at small Knudsen number ε) is required to maintain the apparent value of the kinematic viscosity close to the physical value when using the upwind scheme associated to the first-order updating scheme (14) to simulate the behavior of fluid systems.

The physical value (54) of the kinematic viscosity is always recovered in the incompressible limit if we use the second-order *space centered* finite difference scheme (18) or the *second-order upwind scheme* (19) for approximating the time derivative. Thus, there is no spurious numerical contribution to the kinematic viscosity (i.e., no numerical viscosity) induced by these finite difference LB models which are second order in space.

In the incompressible regime, the apparent value of the kinematic viscosity recovered with the *Lax* scheme is

$$v = \frac{1}{2}\chi c^2\left[2\tau + \frac{(\delta s)^2}{c^2\delta t}\right]. \tag{66}$$

Note that (64) is recovered in the Lax scheme when the condition (3) is satisfied. For the *Lax–Wendroff* and *Beam–Warming schemes*, the apparent value of the kinematic viscosity is identical to (64), even if the condition (3) is no longer required. This value is independent of the lattice spacing but is linearly dependent on the time-step δt, regardless of whether the condition (3) is satisfied or not.

5. Apparent viscosity of the classical LB model

Instead of Eqs. (8), we consider now the slightly modified set of LB evolution equations

$$\partial_t f_i(\mathbf{x},t) + \mathbf{e}_i\cdot\nabla f_i(\mathbf{x},t) = -\frac{1}{\tau}[f_i(\mathbf{x}-\mathbf{e}_i\delta t,t) - f_i^{\mathrm{eq}}(\mathbf{x}-\mathbf{e}_i\delta t,t)] \quad (\sigma = 0,1;\ i = 0,1,\ldots,\mathscr{N}). \tag{67}$$

This set is equivalent to the classical LB equations (1) for a single-component fluid when the first-order upwind finite difference scheme (17) is used and the condition (3) is satisfied. To derive the viscosity formula using the Chapman–Enskog procedure, we make a series expansion of the right-hand side of (67) and express the term $\mathbf{e}_i\nabla f_i(\mathbf{x},t)$ using the first-order upwind scheme (17). The second-order Boltzmann equation with respect to the Knudsen number ε becomes

$$\partial_{t_2} f_i^{(0)} + \partial_{t_1} f_i^{(1)} + e_{i\beta}\partial_{\beta_1} f_i^{(1)} - \frac{1}{2}\frac{\delta s}{c} e_{i\beta}e_{i\gamma}\partial_{\beta_1}\partial_{\gamma_1} f_i^{(0)} = -\frac{1}{\tau}[f_i^{(2)} - \delta t e_{i\beta}\partial_{\beta_1} f_i^{(1)}], \tag{68}$$

while the zeroth- and first-order Boltzmann equations are identical to Eqs. (29) and (30), respectively. Consequently, the apparent kinematic viscosity of this model is

$$v = \frac{1}{2}\chi c^2[2\tau + \frac{\delta s}{c} - 2\delta t]. \tag{69}$$

In the particular case (3) we get

$$v = \frac{1}{2}\chi c^2[2\tau - \delta t], \tag{70}$$

i.e., the well-known viscosity formula of classical LB models (note that in these models, δt is usually set to 1).

6. Numerical results

To check the validity of the viscosity formulae derived in Section 4, we used the attenuation of shear waves whose wavelength equals the system size L. Thus the magnitude of the wavevector is $k = 2\pi/L$. At the initial moment $t = 0$, the velocity field of the fluid was $u_x(x,y,0) = u_0\sin(ky), u_y(x,y,0) = 0$ for $0 \leqslant x,y < L$, where u_0 is a constant. For $u_x := u_x(y,t)$, independent of x, the Navier–Stokes equation (53) becomes

$$\partial_t u_x(y,t) - v\partial_y^2 u_x(y,t) = 0, \tag{71}$$

which admits a solution of the form $u_x(y,t) = u_0\exp(-k^2vt)\sin(ky)$. The apparent value of the kinematic viscosity may be recovered as

$$v = \frac{1}{k^2 t}\log\frac{\mathscr{A}(0)}{\mathscr{A}(t)}, \tag{72}$$

where the Fourier coefficient

$$A(t) = \int_0^L u_x(y,t)\sin(ky)\,\mathrm{d}y = \frac{1}{2}Lu_0\,\mathrm{e}^{-k^2\nu t} \tag{73}$$

is calculated from the numerical results.

We used a lattice of size $L = 1$ for our simulations with periodic boundary conditions. The non-dimensionalized form of the LB evolution equations (8) was used with $c = 1$ and $\tau = 0.01$. To ensure the incompressible limit (small Mach number), we choose $u_0 = 0.01$. The number N of lattice nodes was varied in order to achieve various values of the lattice spacing δs while the time-step was kept constant ($\delta t = 10^{-4}$). As seen in Fig. 1(a), the dependence of the apparent value of the kinematic viscosity vs. the lattice spacing δs is found to be in accordance with the analytical results derived in Section 4. For example, when $N = 500$, we get the values 0.003656, 0.003325 and 0.003342 of the apparent kinematic viscosity in the first-order upwind, space centered and Lax–Wendroff cases, respectively. The relative departure of these values from the theoretically expected values is far below one percent. Moreover, we should point here that the

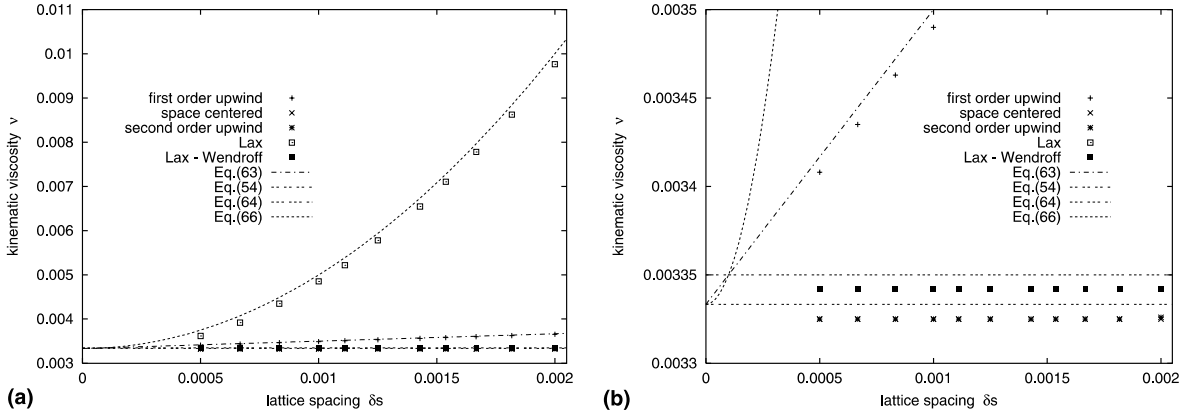

Fig. 1. Dependence of the apparent value of the kinematic viscosity ν vs. lattice spacing δs for $\tau = 0.01$ and $\delta t = 0.0001$.

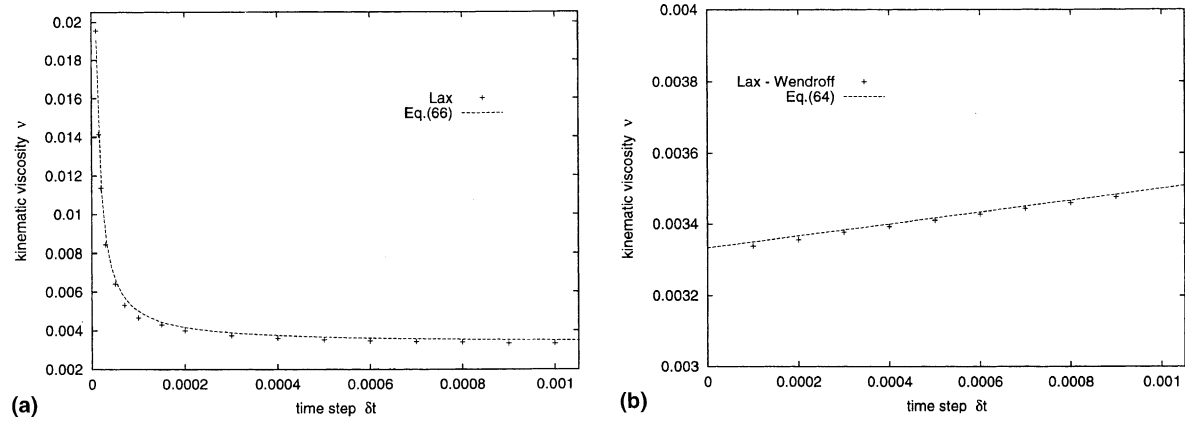

Fig. 2. Dependence of the apparent value of the kinematic viscosity ν vs. time-step δt for $\tau = 0.01$ and $\delta s = 0.001$: (a) Lax scheme; (b) Lax–Wendroff scheme (+, numerical results; lines, analytical solutions).

difference between the values of the apparent viscosity recovered using the Lax–Wendroff scheme and the values recovered using the space centered and the second-order upwind schemes is in good agreement with Eq. (64). This is evident also in Fig. 1(b), which is an enlarged portion of Fig. 1(a). Fig. 2 shows the dependence of the apparent value of the kinematic viscosity vs. time-step δt for the Lax and Lax–Wendroff schemes, for constant lattice spacing ($\delta s = 0.001$). Good agreement between numerical results and corresponding analytical formulae is clearly seen.

We also explored shear waves of shorter wavelength in the incompressible regime, namely with $k' = nk$, where n is an integer. This introduces a factor of n^2 into the exponential damping factor, so that $\exp(-k^2 \nu t)$ in (73) is replaced by $\exp(-k^2 n^2 \nu t)$. Good agreement with simulations is still obtained so long as $\delta s \ll L/n$, but of course spatial resolution is lost if n becomes too large.

7. Conclusions

Finite difference LB models, Eqs. (14)–(22), may be appropriate for the general case, Eqs. (5)–(7), of multicomponent fluid systems (when the masses of particles are different and the thermal speeds (4) of each species of particles are not identical) only if certain conditions are satisfied. These conditions are provided by the requirement of correct mass and momentum equations to be recovered using these models.

From the six FDLB schemes introduced in Section 2 in order to compute the term $\mathbf{e}_i \cdot \nabla f_i(\mathbf{x}, t)$ in the LB equations (8), the characteristic based schemes (first-order upwind, Lax, Lax–Wendroff and Beam–Warming) cannot achieve the correct mass equation in the compressible regime (even for CFL = 1) when associated to the updating procedures (15) and (16), which are second order in time. In order to get the correct mass equation for the four spatial schemes mentioned above, one can use the forward Euler updating rule (14). Then there is no correction to the mass equation for the Lax–Wendroff and the Beam–Warming schemes. However, the CFL = 1 condition is needed in the compressible regime to eliminate a correction for the first-order upwind scheme and the Lax scheme (this condition is no longer required in the incompressible limit). The opposite holds for the space centered and the second-order upwind schemes: to recover the correct mass equation in the compressible regime, one of the second-order updating rules (15) or (16) should be used instead.

All FDLB schemes investigated in this paper give the correct Navier–Stokes equation in the incompressible limit. However, FDLB schemes may introduce a spurious numerical viscosity which is always added to the physical value of the kinematic viscosity $\nu = \tau \chi c^2$ to get an apparent value of this quantity. The apparent values of the kinematic viscosity we derived in the incompressible limit (see Eq. (62) and Table 1) are characteristic to each FD scheme used to compute the term $\mathbf{e}_i \cdot \nabla f_i(\mathbf{x}, t)$ in the LB equations (8), regardless the FD scheme used for the time derivative. No numerical viscosity is introduced in the incompressible limit when using two particular finite difference schemes: the space centered scheme (18) and the second-order upwind scheme (19).

The classical LB model is recovered as a very special case of the upwind finite difference LB model, when also the relaxation term is calculated on the characteristics line. The condition $\tau > \delta t/2$, which is required by the classical LB model in order to get a positive value of the kinematic viscosity during simulations is no longer required in characteristics based finite difference LB models.

Acknowledgements

This work was supported by the US Air Force European Office for Aerospace Research and Development (EOARD) under contract F61775-98-WE101 (1998–1999), NASA Microgravity Research Division NAG 8-1704 (2000–2001) and the Romanian Space Agency under contract 544 (2000–2001).

References

[1] P. Bhatnagar, E.P. Gross, M. Krook, A model for collision processes in gases I: small amplitude processes in charged and neutral one-component systems, Phys. Rev. 94 (1954) 511.
[2] P. Welander, On the temperature jump in a rarefied gas, Arkiv för Fysik 7 (1954) 507.
[3] X. He, L.S. Luo, A priori derivation of the lattice Boltzmann equation, Phys. Rev. E 55 (1997) R6333.
[4] X. He, L.S. Luo, Theory of the lattice Boltzmann method: from the Boltzmann equation to the lattice Boltzmann equation, Phys. Rev. E 56 (1997) 6811.
[5] D.H. Rothman, S. Zaleski, Lattice Gas Cellular Automata: Simple Models of Complex Hydrodynamics, Cambridge University Press, Cambridge, 1997.
[6] S. Chen, G.D. Doolen, Lattice Boltzmann method for fluid flows, Annu. Rev. Fluid Mech. 30 (1998) 329.
[7] B. Chopard, M. Droz, Cellular Automata Modeling of Physical Systems, Cambridge University Press, Cambridge, 1999.
[8] D.A. Wolf-Gladrow, Lattice Gas Cellular Automata and Lattice Boltzmann Models, Springer Verlag, Berlin, 2000.
[9] Y.H. Qian, D. D'Humières, P. Lallemand, Lattice BGK models for Navier–Stokes equation, Europhys. Lett. 17 (1992) 479.
[10] L.S. Luo, Theory of the lattice Boltzmann method: lattice Boltzmann models for nonideal gases, Phys. Rev. E 62 (2000) 4982.
[11] N. Cao, S. Chen, S. Jin, D. Martinez, Physical symmetry and lattice symmetry in the lattice Boltzmann method, Phys. Rev. E 55 (1997) R21.
[12] R. Mei, W. Shyy, On the finite difference-based lattice Boltzmann method in curvilinear coordinates, J. Comput. Phys. 143 (1998) 426.
[13] V. Sofonea, Lattice Boltzmann models for multicomponent fluids, Final Report (contract No. F61775-98-WE101), Institute for Complex Fluids, Polytechnical University of Timişoara, 1999 (unpublished).
[14] T. Seta, K. Kono, D. Martinez, S. Chen, Lattice Boltzmann scheme for simulating two-phase flows, JSME Int. J. Ser. B 43 (2000) 305.
[15] T.H. Lee, C.L. Lin, A characteristic Galerkin method for discrete Boltzmann equation, J. Comput. Phys. 171 (2001) 336, doi:10.1006/jcph.2001.6791.
[16] W.H. Press, S.A. Teukolsky, W.T. Vetterling, B.P. Flannery, Numerical Recipes in Fortran 77: The art of Scientific Computing, second ed., Cambridge University Press, Cambridge, 1992.
[17] K.A. Hoffmann, S.T. Chiang, Computational Fluid Dynamics, third ed., Engineering Education System, Wichita, Kansas, 1998.
[18] E.F. Toro, Riemann Solvers and Numerical Methods for Fluid Dynamics, second ed., Springer Verlag, Berlin, 1999.
[19] H. Grad, On the kinetic theory of rarefied gases, Comm. Pure Appl. Math. 2 (1949) 331.
[20] J.M. Burgers, Flow Equations for Composite Gases, Academic Press, New York, 1969.
[21] V. Sofonea, R.F. Sekerka, BGK models for diffusion in isothermal binary fluid systems, Physica A 299 (2001) 494.